Characterization of Lanthanide(III) DOTP Complexes: Thermodynamics, Protonation, and Coordination to Alkali Metal Ions

A. D. Sherry,*,†,‡ J. Ren,† J. Huskens,† E. Brücher,§ É. Tóth,§ C. F. C. G. Geraldes,|| M. M. C. A. Castro,|| and W. P. Cacheris†,⊥

Department of Chemistry, University of Texas at Dallas, P.O. Box 830688, Richardson, Texas 75083-0688, The Mary Nell and Ralph B. Rogers Magnetic Resonance Center, Department of Radiology, University of Texas Southwestern Medical Center, 5801 Forest Park Road, Dallas, Texas 75235-9085, Department of Inorganic & Analytical Chemistry, Lajos Kossuth University, H-4010 Debrecen, Hungary, Department of Biochemistry, Faculty of Science & Technology, University of Coimbra, 3049 Coimbra, Portugal, and The Mattson Jack Group, Suite 180, 11960 Westline Industrial Drive, St. Louis, Missouri 63146

Received January 18, 1996[⊗]

Several solution properties of complexes formed between the trivalent lanthanide ions (Ln^{III}) and the macrocyclic ligand $DOTP^{8-}$, including stability constants, protonation equilibria, and interactions of the $LnDOTP^{5-}$ complexes with alkali metal ions, have been examined by spectrophotometry, potentiometry, osmometry, and ^{1}H, ^{31}P, and ^{23}Na NMR spectroscopy. Spectrophotometric competition experiments between DOTP and arsenazo III for complexation with the Ln^{III} ions at pH 4 indicate that the thermodynamic stability constants (log K_{ML}) of $LnDOTP^{5-}$ range from 27.6 to 29.6 from La^{III} to Lu^{III}. The value for $LaDOTP^{5-}$ obtained by colorimetry (27.6) was supported by a competition experiment between DOTP and EDTA monitored by ^{1}H NMR (27.1) and by a potentiometric competition titration between DTPA and DOTP (27.4). Potentiometric titrations of several $LnDOTP^{5-}$ complexes indicated that four protonation steps occur between pH 10 and 2; the protonation constants determined by potentiometry were consistent with ^{31}P shift titrations of the $LnDOTP^{5-}$ complexes. Dissection of the ^{31}P shifts of the heavy $LnDOTP^{5-}$ complexes (Tb → Tm) into contact and pseudocontact contributions showed that the latter dominated at all pH values. The smaller ^{31}P shifts observed at lower pH for $TmDOTP^{5-}$ were partially due to relaxation of the chelate structure which occurred upon protonation. The ^{31}P shifts of other $LnDOTP^{5-}$ complexes (Ln = Pr, Nd, Eu) showed a different pH-dependent behavior, with a change in chemical shift direction occurring after two protonation steps. This behavior was traced to a pH-dependent alteration of the contact shift at the phosphorus nuclei as these complexes were protonated. ^{23}Na NMR studies of the interactions of $TmDOTP^{5-}$ with alkali and ammonium cations showed that Et_4N^+ and Me_4N^+ did not compete effectively with Na^+ for the binding sites on $TmDOTP^{5-}$, while K^+ and NH_4^+ competed more effectively and Cs^+ and Li^+ less effectively. A ^{23}Na shift of more than 400 ppm was observed at low $Na^+/TmDOTP^{5-}$ ratios and high pH, indicating that Na^+ was bound near the 4-fold symmetry axis of $TmDOTP^{5-}$ under these conditions. Osmolality measurements of chelate samples containing various amounts of Na^+ indicated that at high $Na^+/TmDOTP^{5-}$ ratios at least three Na^+ ions were bound to $TmDOTP^{5-}$. These ions showed a significantly smaller ^{23}Na-bound shift, indicating they must bind to the chelate at sites further away from the 4-fold symmetry axis. Fully bound ^{23}Na shifts and relaxation rate enhancements and binding constants for all $Na_xH_yTmDOTP$ species were obtained by fitting the observed ^{23}Na shift and relaxation data and the osmometric data, using a spreadsheet approach. This model successfully explained the ^{23}Na shift and osmolality observed for the commercial reagent $Na_4HTmDOTP{\cdot}3NaOAc$ (at 80 mM at pH 7.4).

Introduction

Stable lanthanide chelates of polyazamacrocyclic ligands are finding wide applications in biomedical NMR, including uses as paramagnetic shift reagents (SRs) for spectroscopic studies of NMR-active cations[1] and water relaxation or contrast agents (CAs) for magnetic resonance imaging.[2−4] The lanthanide complexes of 1,4,7,10-tetraazacyclododecane-1,4,7,10-tetrakis-(methylenephosphonic acid) (H_8DOTP) have been studied in some detail with regard to their solution and magnetic properties[5−8] and as high-resolution NMR shift reagents for

* To whom correspondence should be addressed at the University of Texas at Dallas. Telephone: 214-883-2907 or 214-648-5877. FAX: 214-883-2925 or 214-648-5881. E-Mail: sherry@utdallas.edu.
† University of Texas at Dallas.
‡ University of Texas Southwestern Medical Center.
§ Lajos Kossuth University.
|| University of Coimbra.
⊥ The Mattson Jack Group.
⊗ Abstract published in *Advance ACS Abstracts,* July 1, 1996.

(1) Sherry, A. D.; Geraldes, C. F. G. C. Shift Reagents in NMR Spectroscopy. In: *Lanthanide Probes in Life, Chemical and Earth Sciences*: *Theory and Practice*; Bünzli, J.-C. G, Choppin, G. R., Eds.; Elsevier: Amsterdam, 1989; pp 93−126.
(2) Lauffer, R. B. *Chem. Rev.* **1987**, *87*, 901−927.
(3) Sherry, A. D. *J. Less-Commun. Met.* **1989**, *149*, 133−141.
(4) Tweedle, M. F. Relaxation Agents in NMR Imaging. In: *Lanthanide Probes in Life, Chemical and Earth Sciences: Theory and Practice*; Bünzli, J.-C. G., Choppin, G. R., Eds; Elsevier: Amsterdam, 1989; pp 127−179.
(5) Geraldes, C. F. G. C.; Sherry, A. D.; Kiefer, G. E. *J. Magn. Reson.* **1992**, *97*, 290−304.
(6) Sherry, A. D.; Geraldes, C. F. C. G.; Cacheris, W. P. *Inorg. Chim. Acta* **1987**, *139*, 137−139.
(7) Aime, S.; Botta, M.; Terreno, E.; Anelli, P. L.; Uggeri, F. *Magn. Reson. Med*. **1993**, *30*, 583−591.
(8) Geraldes, C. F. G. C.; Brown, R. D., III; Cacheris, W. P.; Koenig, S. H.; Sherry, A. D.; Spiller, M. *Magn. Reson. Med*. **1989**, *9*, 94−104.

S0020-1669(96)00059-6 CCC: $12.00

proteins.[9,10] The thulium complex has proved to be particularly favorable as a cation (^{23}Na, ^{7}Li, ^{133}Cs) shift reagent in NMR studies of isolated cells,[11−13] perfused tissues,[14−18] and intact animals.[19−22] $TmDOTP^{5-}$ induces a particularly large paramagnetic shift in cation nuclei that ion-pair with the SR in physiological media plus has the advantage of having a lower bulk paramagnetic susceptibility than dysprosium-based SRs. This combination of properties has been shown to be key[20,22] for achieving baseline resolution of intra- and extracellular ^{23}Na resonances in heterogeneous *in vivo* tissue. The frequency shift induced in any NMR-active cation that forms an ion-pair complex with a paramagnetic $LnDOTP^{5-}$ complex in aqueous solution is known to be pH dependent due to competition of H^+ at the coordinated side-chain phosphonate groups.[11,13,14] The ^{31}P NMR chemical shift *versus* pH titration curve for $DyDOTP^{5-}$ was interpreted as reflecting protonation of two bound phosphonate groups between pH 8 and 3.[11]

We have now reinvestigated the protonation equilibria of the $LnDOTP^{5-}$ complexes and herein report potentiometric titrations for several of the complexes, ^{31}P NMR chemical shift *versus* pH data for two complexes (to illustrate differences in complexes whose shifts are dominated by contact *versus* pseudocontact mechanisms), and thermodynamic stability constants for the entire lanthanide series. Dissection of the ^{31}P shifts of the heavy $LnDOTP^{5-}$ complexes (Tb → Tm) into contact and pseudocontact contributions show that the latter dominate at all pH values. We show that the smaller ^{31}P shifts observed at low pH for $TmDOTP^{5-}$ partially reflect relaxation of the chelate structure. We have also investigated alkali cation binding to $TmDOTP^{5-}$ in some detail using both paramagnetic induced shift and relaxation rate measurements and show that these data are consistent with an equilibrium model involving a single cation binding site on or near the 4-fold symmetry axis of the complex at low $Na^+/TmDOTP^{5-}$ ratios and three to four cation binding sites further away from the 4-fold axis of symmetry at higher $Na^+/TmDOTP^{5-}$ ratios. This cation-binding model accurately predicts the number of unassociated species in solution as detected by vapor pressure osmometry.

Experimental Section

Potentiometry. All potentiometric titrations were performed in a jacketed vessel at 25.0 ± 0.1 °C under a N_2 atmosphere using a cup volume of 5−10 mL. The ionic strength of all samples was adjusted to 0.1 M prior to titration using Me_4NCl. Hydrogen ion concentrations were calculated from the measured pH values using the method proposed by Irving *et al.*[23] The titrations were evaluated using either a spreadsheet program[24] or the computer program PSEQUAD.[25] The protonation constants of DOTP redetermined by potentiometric titration of 4.6 mM H_8DOTP (I = 0.1 M, Me_4NCl) with 0.1 M Me_4NOH (see Figure 3) agreed well with data obtained previously.[26,27] The protonation constants of $LnDOTP^{5-}$ (Ln = Ce, Nd, Gd, Tm, Lu) were determined in 0.1 M Me_4NCl by titration of 5 mM $(Me_4N)_5LnDOTP$ with 0.2 M HCl (see Table 1). Two separate titrations, with 25 data points from pH 3.5 to 9, were performed for each complex.

A $LaDOTP^{5-}$ stability constant was determined by a potentiometric competition experiment in which a 1.10 mM $LaCl_3$ + 1.10 mM $(Me_4N)_8DOTP$ + 1.11 mM $(Me_4N)_5DTPA$ (5 mL) mixture was titrated with 0.1 M HCl (see Figure 4). The pK_a values of $DTPA^{5-}$ as well as the stability constant of $LaDTPA^{2-}$ in 0.1 M Me_4NCl were obtained from the literature.[28] This titration was performed allowing between 30 and 180 s for equilibration after each addition of titrant.

Colorimetry. Spectrophotometric competition titrations of lanthanide(III) cations, arsenazo III (99.9%, Aldrich Chemical Co.), and the ligand H_8DOTP (prepared as recently described[29]) were carried out in 0.01 M acetate buffer (pH 4) containing $(3-6) \times 10^{-5}$ M arsenazo III and 0.1 M NaCl to maintain constant ionic strength (since Na^+ does not bind to DOTP to any significant extent at this pH, the presence of NaCl to maintain ionic strength has no effect upon the thermodynamic stability constants calculated from these data). All absorbance measurements were made on an HP-8450A linear diode-array spectrophotometer after the solutions had reached equilibrium (several days). The pH 4 conditional $LnDOTP^{5-}$ formation constants were obtained from the absorbance values using a computational method described previously.[30] Thermodynamic stability constants were obtained from these data by correcting for direct proton competition for the ligand and for protonation of each $LnDOTP^{5-}$ complex. The relevant equations include ($M = Ln^{3+}$, $L = DOTP^{8-}$)

$$K_{ML} = [ML]/[M][L] \quad (1)$$

$$K_{cond} = [ML]_T/[M][L]_T \quad (2)$$

where

$$[ML]_T = \Sigma_n[H_nML] \quad (n = 0-4) \quad (3)$$

$$[L]_T = \Sigma_n[H_nL] \quad (n = 0-8) \quad (4)$$

These equations may be simplified to

$$K_{ML} = K_{cond}{*}\alpha_L/\alpha_{ML} \quad (5)$$

where

(9) Dick, L. R.; Geraldes, C. F. G. C.; Sherry, A. D.; Gray, C. W.; Gray, D. M. *Biochemistry* **1989**, *28*, 7896−7904.
(10) Swinkels, D. W.; van Duynhoven, J. P. M.; Hilbers, C. W.; Tesser, G. I. *Recl. Trav. Chim. Pays-Bas* **1991**, *110*, 124−128.
(11) Sherry, A. D.; Malloy, C. R.; Jeffrey, F. M. H.; Cacheris, W. P.; Geraldes, C. F. G. C. *J. Magn. Reson.* **1988**, *76*, 528−533.
(12) Wittenkeller, L.; Mota de Freitas, D.; Geraldes, C. F. G. C.; Tomé, A. J. R. *Inorg. Chem.* **1992**, *31*, 1135−1144.
(13) Ramasamy, R.; Mota de Freitas, D.; Jones, W; Wezeman, F.; Labotka, R.; Geraldes, C. F. G. C. *Inorg. Chem.* **1990**, *29*, 3979−3985.
(14) Buster, D. C.; Castro, M. M. C. A.; Geraldes, C. F. G. C.; Malloy, C. R.; Sherry, A. D.; Siemers, T. C. *Magn. Reson. Med.* **1990**, *15*, 25−32.
(15) Malloy, C. R.; Buster, D. C.; Castro, M. M. C. A.; Geraldes, C. F. G. C.; Jeffrey, F. M. H.; Sherry, A. D. *Magn. Reson. Med.* **1990**, *15*, 33−44.
(16) Butwell, N. B.; Ramasamy, R.; Sherry, A. D.; Malloy, C. R. *Invest. Radiol.* **1991**, *26*, 1079−1082.
(17) Butwell, N. B.; Ramasamy, R.; Lazar, I.; Sherry, A. D.; Malloy, C. R. *Am. J. Physiol.* **1993**, *264*, H1884−H1889.
(18) Pike, M. M.; Su Luo, C.; Clark, M. D.; Kirk, K. A.; Kitakaze, M.; Madden, M. C.; Cragoe, E. J., Jr.; Pohost, G. M. *Am. J. Physiol.* **1993**, *265*, H2017−H2026.
(19) Bansal, N.; Germann, M. J.; Lazar, I.; Malloy, C. R.; Sherry, A. D. *J. Magn. Reson. Imag.* **1992**, *2*, 385−391.
(20) Bansal, N.; Germann, M. J.; Seshan, V.; Shires, G. T., III; Malloy, C. R.; Sherry, A. D. *Biochemistry* **1993**, *32*, 5638−5643.
(21) Xia, Z.-F.; Horton, J. W.; Zhao, P.-Y.; Bansal, N.; Babcock, E. E.; Sherry, A. D.; Malloy, C. R. *J. Appl. Physiol.* **1994**, *76*, 1507−1511.
(22) Seshan, V.; Germann, M. J.; Preisig, P.; Malloy, C. R.; Sherry, A. D.; Bansal, N. *Magn. Reson. Med.* **1995**, *34*, 25−31.
(23) Irving, H. M.; Miles, M. G.; Pettit, L. *Anal. Chim. Acta* **1967**, *38*, 475.
(24) Huskens, J.; Van Bekkum, H.; Peters, J. A. *Comput. Chem.* **1995**, *19*, 409−416.
(25) Zekany, L.; Nagypal, I. In: *Computational Methods for Determination of Formation Constants*; Leggett, D. J., Ed.; Plenum: New York, 1985; p 291.
(26) Geraldes, C. F. G. C.; Sherry, A. D.; Cacheris, W. P. *Inorg. Chem.* **1989**, *28*, 3336−3341.
(27) Delgado, R.; Siegfried, L. C.; Kaden, T. A. *Helv. Chim. Acta* **1990**, *73*, 140−148.
(28) Martell, A. E.; Smith, R. M. *Critical Stability Constants*; Plenum: New York, 1975; Vol. 4.
(29) Lazar, I.; Hrncir, D. C.; Kim, W.-D.; Kiefer, G. E.; Sherry, A. D. *Inorg. Chem.* **1992**, *31*, 4422−4424.
(30) Sherry, A. D.; Cacheris, W. P.; Kuan, K.-T. *Magn. Reson. Med.* **1988**, *8*, 180−190.

$$\alpha_L = 1 + K_1^L[H] + K_1^L K_2^L[H]^2 + K_1^L K_2^L K_3^L[H]^3 + ... \quad (6)$$

$$\alpha_{ML} = 1 + K_1^{ML}[H] + K_1^{ML} K_2^{ML}[H]^2 + K_1^{ML} K_2^{ML} K_3^{ML}[H]^3 + K_1^{ML} K_2^{ML} K_3^{ML} K_4^{ML}[H]^4 \quad (7)$$

K_n^{ML} (=$[H_nML]/[H_{n-1}ML][H]$) represent protonation constants of $LnDOTP^{5-}$ (Table 1) while K_n^L (=$[H_nL]/[H_{n-1}L][H]$) represent protonation constants of $DOTP^{8-}$ as measured by potentiometry[26] (K_2-K_6) in 0.1 M tetramethylammonium chloride and by NMR[27] (K_1) in tetramethylammonium nitrate.

NMR. $LnDOTP^{5-}$ solutions were prepared for NMR pH titration by mixing a solution of H_8DOTP dissolved in D_2O and neutralized with either NaOD (for ^1H NMR) or Me_4NOH (for ^{31}P NMR) with a stoichiometric amount of $LnCl_3$. After the complex was fully formed (as evidenced by stabilization of the pH), each complex was adjusted to high pH with either NaOD or Me_4NOH and then titrated to low pH with DCl while the ^1H or ^{31}P spectrum was monitored. The pD values measured potentiometrically were converted to pH values (pH = pD − 0.4) before plotting the data. ^{23}Na spin−lattice relaxation rate and chemical shift titrations with NaCl were carried out in D_2O starting with 15 mM $TmDOTP^{5-}$ as the tetramethylammonium salt. All NMR measurements (^{23}Na, ^{31}P, and ^1H) were recorded on a GN-500 spectrometer. ^1H chemical shifts were referenced to *tert*-butyl alcohol as an internal standard, ^{31}P chemical shifts were referenced to 85% H_3PO_4 as an external standard, and ^{23}Na chemical shifts were referenced to normal saline as an external standard.

For the NMR determination of the $LaDOTP^{5-}$ stability constant, solutions of DOTP (pH 8) were mixed with varying amounts of $LaCl_3$ and Na_2H_2EDTA. After gentle evaporation, the salts were redissolved in D_2O and allowed to equilibrate for 3−5 days at room temperature. During this equilibration period, the pH was adjusted occasionally with NaOH to maintain a pH value between 7 and 8, a range which provided resolution of the ^1H signals of free and bound EDTA and free and bound DOTP at 500 MHz. A 20 s interpulse delay was used to record each of these spectra.

Vapor Pressure Osmometry. Solution osmolalities were measured on a Wescor vapor pressure osmometer (Model No. 5500) at room temperature. Samples were prepared as described above for the NMR experiments.

Species Calculations and Curve-Fit Procedures. The experimental data (^{23}Na shifts, osmometry, potentiometry) were fitted to various binding models by using the Solver feature of Microsoft Excel. The experimental NMR data obtained at pH 10.7 were first used to optimize the $Na_xTmDOTP$ binding constants and limiting shifts, assuming a statistical decrease in the stepwise binding constants for the B-sites. Then, the pH 7.4 NMR data and the potentiometric data were included to evaluate the protonation constants for the mixed $Na_xH_yTmDOTP$ species, which were constrained to be less than the corresponding values for Na^+-free $H_yTmDOTP$ species obtained by potentiometry (see Table 1).

Results

^{31}P NMR Chemical Shifts. The ^{31}P chemical shifts of $EuDOTP^{5-}$ and $TmDOTP^{5-}$ are shown as a function of pH in Figure 1. A single phosphorus resonance was observed over the entire pH range for both complexes, indicating that all protonated and deprotonated species were in fast exchange. Protonation of $TmDOTP^{5-}$ began near pH 8.5, as evidenced by deshielding of the phosphorus resonance of the complex, and continued until approximately pH 4.0. The complex remained intact to well below pH 2 (at least for several hours after pH adjustment) as evidenced by the absence of a free ligand signal near 0 ppm. Protonation of $EuDOTP^{5-}$ also resulted in a deshielding of the phosphorus nucleus of this complex beginning near pH 8.5. This continued to nearly pH 5.7, whereupon an abrupt change in direction of the shift was observed as the pH was lowered further. Protonation was complete by pH 2.5, and again, this complex remained intact well below this pH. Both complexes did show partial dissociation into free lanthanide and free ligand after storage at low pH for several days. The ^{31}P chemical shift (δ) *versus* pH curves for diamagnetic $LaDOTP^{5-}$ and $LuDOTP^{5-}$ had the same general shape (data not shown) as that illustrated for $TmDOTP^{5-}$, but in these cases the $\Delta\delta$ between pH 10 and 2 amounted to only 2.8 and 2.6 ppm, respectively. The corresponding curves for complexes of Ce, Tb, Dy, Ho, Er, and Yb had the same shape as that illustrated for $TmDOTP^{5-}$ while the curves for the Pr and Nd complexes had the same biphasic shape as that illustrated for $EuDOTP^{5-}$.

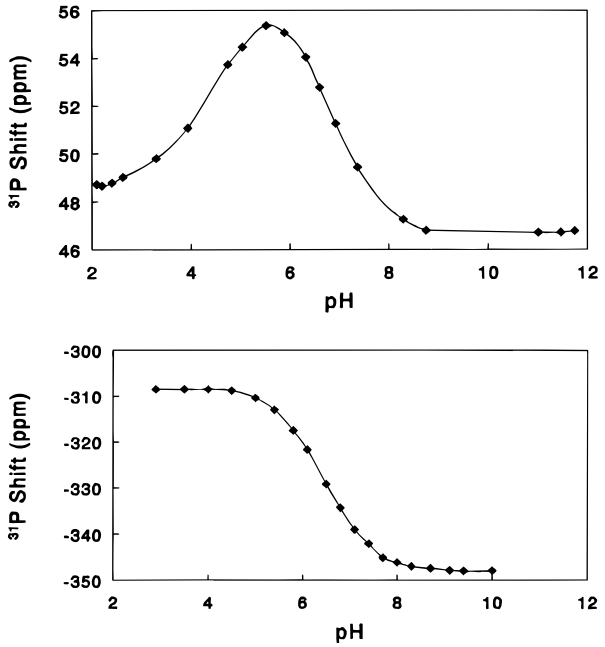

Figure 1. ^{31}P chemical shifts of $EuDOTP^{5-}$ (top) and $TmDOTP^{5-}$ (bottom) as a function of pH.

^{31}P chemical shifts for the entire series of $LnDOTP^{5-}$ complexes have been reported previously[5,6] at a single pH value of 10. An analysis of those ^{31}P shifts indicated that the heavy lanthanide complexes (Tb → Yb) were dominated by pseudocontact contributions while the lighter lanthanide complexes (Ce → Eu) had significant contact contributions.[5] Thus, one possible interpretation of the $TmDOTP^{5-}$ data shown in Figure 1 is that the pseudocontact shift induced by paramagnetic Tm^{3+} became progressively smaller as the complex was protonated (only 2.7 ppm of the total $\Delta\delta$ of 40 ppm reflects deshielding of the phosphorus nucleus due to protonation), perhaps due to relaxation of its structure and slight movement of the coordinated phosphonate ligands away from the paramagnetic metal center. Similar behavior was noted for $EuDOTP^{5-}$ above pH 5.5, while below this pH, the ^{31}P resonances shifted in the opposite direction, perhaps due to an increase in the contact term at lower pH values.

This hypothesis was tested by measuring the ^{31}P chemical shifts of the $LnDOTP^{5-}$ complexes at pH 3 and 7. Plots of lanthanide-induced shift (LIS)/$\langle S_z\rangle$ *versus* $D/\langle S_z\rangle$ (see Supporting Information) for the heavy $LnDOTP^{5-}$ complexes indicate that both the pseudocontact shifts and the hyperfine coupling constants fall in the order pH 3 < pH 7 < pH 10. Quantitatively, the pseudocontact term (slope) decreases by 10% over this pH range while the contact term (intercept) decreases by nearly 20%; however, the pseudocontact shift of the phosphorus dominated the contact shift at all three pH values. Thus, we conclude that the pH dependence shown in Figure 1 for $TmDOTP^{5-}$ largely results from a smaller pseudocontact shift at the low pH values.

Table 1. Protonation Constants[a] of the $LnDOTP^{5-}$ Complexes As Determined by Potentiometric Titrations in 0.1 M Me_4NCl, at 25 °C

Ln	log K_1	log K_2	log K_3	log K_4
Ce	7.7	6.7	5.6	4.7
Nd	7.9	6.6	5.6	4.4
Gd	7.6	6.3	5.4	4.0
Tm	8.3	6.9	5.6	4.5
Lu	8.7	7.0	5.5	4.0
av	8.0	6.7	5.5	4.3

[a] The standard deviation in each constant was ±0.1, based upon two separate titrations.

The corresponding LIS/$\langle S_z \rangle$ *versus* $D/\langle S_z \rangle$ plots of the ^{31}P shift data for the lighter $LnDOTP^{5-}$ complexes have slopes near zero (data not shown), indicating that these shifts are dominated by contact interactions. The amount of scatter in these relationships for these ions does not allow a quantitative separation of the pseudocontact term, but its contribution appears to be minor. Consequently, the abrupt change in direction of the measured ^{31}P shifts for $EuDOTP^{5-}$ (and the Pr and Nd complexes) with decreasing pH (Figure 1) likely reflects a pH-dependent change in the contact shift as the complex becomes protonated. The direction of these shifts suggests that the Eu−O−P bond network becomes more covalent as the first two phosphonates are protonated and then becomes less covalent once again below pH 5.7 during the third and fourth protonations. $CeDOTP^{5-}$ does not show the same titration behavior as the Pr, Nd, and Eu complexes probably because its contact term is much smaller than its pseudocontact term at all pH values.[1]

Potentiometric Titrations. pH titrations of several $LnDOTP^{5-}$ complexes were performed using standard potentiometric methods at a constant ionic strength of 0.1 M (Me_4NCl). These data indicated that four protonations occur between pH 10 and 2 in each of the complexes. A fitting of the titration data to the simplest model involving four sequential protonations of a monomeric $LnDOTP^{5-}$ complex gave the protonation constants reported in Table 1. These values were consistent with the shifts observed in the ^{31}P NMR spectra as function of pH, indicating that the ^{31}P shifts indeed reflected protonation of the four coordinated phosphonates. This differed from the model reported earlier[11] for $DyDOTP^{5-}$ derived from its pH *versus* ^{31}P chemical shift curve. A speciation curve generated using the constants listed in Table 1 (not shown) indicates that $HTmDOTP^{4-}$ is the major species present in aqueous solution at a physiological pH of 7.4 (70%), while $TmDOTP^{5-}$ and $H_2TmDOTP^{3-}$ contribute about 11 and 19%, respectively.

Direct potentiometric titration of a stoichiometric mixture of a lanthanide salt and H_8DOTP to obtain a thermodynamic stability constant is problematical because complexation is a relatively slow process and precipitation of insoluble Ln^{3+}−phosphonate complexes (where the cation is not chelated by the macrocyclic nitrogens of DOTP) or hydroxides occurs above pH 6. When a 1/1 mixture of La^{3+} and H_8DOTP was titrated with aqueous base, the solution became cloudy between pH 6 and 7.5 but cleared again at higher pH values. A well-defined end point was seen at exactly 8 equiv of base (Figure 2). Similar results were obtained when DOTP was titrated in the presence of 1 equiv of $CuCl_2$ (data not shown). The last end point that was apparent in the titration curve of the free ligand occurred at about pH 10, after 6 equiv of base had been added. These data indicate that DOTP has two pK_a's above pH 10, contrary to a single high pK_a of 12.5 determined previously by potentiometry.[26] The potentiometric titration data for the free ligand (Figure 1) could be fit to six protonation steps (1.77 ± 0.06, 5.17 ± 0.02, 6.17 ± 0.03, 8.01 ± 0.02, 9.25 ± 0.03, and 12.5 ± 0.1, essentially the same as those reported previously[26]). Even

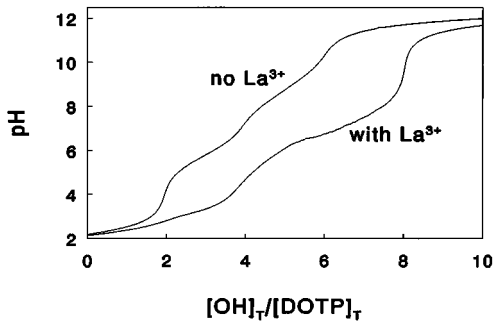

Figure 2. Potentiometric titration curves of 4.6 mM H_8DOTP titrated with 0.1 M Me_4NOH in the absence and presence of 1 equiv of La^{3+} (I = 0.1 M, Me_4NCl)

at the highest pH of this titration, the ligand was partially protonated (~25% HL and 75% H_2L at pH 12). Delgado *et al.*[27] reported a value of 13.7±0.1 (as determined by ^1H NMR) for the highest protonation constant of $DOTP^{8-}$. Although their NMR titration was done in the presence of Me_4N^+, the ionic strength was by necessity changing and much higher (>1 M) than during our potentiometric titration. Nevertheless, as it is methodologically impossible to verify the highest protonation constant by potentiometry and our Cu^{2+} and La^{3+} titrations verified that an additional high pK_a must be present, we used the value of log K_1 = 13.7 ± 0.1 along with the remaining potentiometrically determined values in 0.1 M Me_4NCl for all subsequent thermodynamic calculations.

Stability Constants of the $LnDOTP^{5-}$ Complexes. Given the experimental difficulties of performing standard potentiometric titrations of DOTP with a trivalent lanthanide cation, we have measured the stability constants of several $LnDOTP^{5-}$ complexes using three different methods. The first involves measurement of conditional stability constants for these complexes using the same spectrophotometric technique as used previously[31] for obtaining the $LnDOTA^-$ stability constants. This method involves competition between the colorimetric dye arsenazo III and DOTP for a Ln^{3+} cation in acetate buffer at pH 4.[30] Several solutions were prepared containing known amounts of Ln^{3+}, DOTP, and arsenazo III, and these were allowed to equilibrate at pH 4 and room temperature for several days to ensure complete equilibration. Once the absorbance values were steady, final readings were taken and a pH 4 conditional stability constant was evaluated. These are reported for 13 lanthanide complexes in Table 2A. Since there was no obvious trend in the protonation constants of the complexes listed in Table 1, an average for each protonation constant of the five different $LnDOTP^{5-}$ complexes was used in the calculation of α_{ML}. Similarly, the ligand protonation constants as determined by potentiometry and NMR were used in the calculation of α_L. The resulting thermodynamic stability constants, K_{ML} (calculated using eq 5), are listed in Table 2A.

The second method used ^1H NMR spectroscopy to monitor competition between EDTA and DOTP for a known quantity of La^{3+}. Several samples were prepared containing differing amounts of La^{3+}, DOTP, and EDTA, a ligand with well characterized pK_a's and complex stability constants. These were allowed to equilibrate at room temperature for periods of up to 1 week to ensure equilibration, and NMR spectra of the samples were recorded at various times during this period to assess the equilibration process. After complete equilibration, the areas of the ethylenediamine singlet in $LaEDTA^-$ at 2.7 ppm and a multiplet consisting of two ethylenediamine protons and one

(31) Cacheris, W. P.; Nickle, S. K.; Sherry, A. D. *Inorg. Chem.* **1987**, *26*, 958−960.

Table 2. Conditional and Thermodynamic Stability Constants for the $LnDOTP^{5-}$ Complexes

A. Values Measured by Colorimetry at pH 4 (Competition with Arsenazo III (See Text))[a]

Ln	log K_{cond} (M^{-1}) (±0.2)	log K_{ML} (M^{-1}) (±0.3)	Ln	log K_{cond} (M^{-1}) (±0.2)	log K_{ML} (M^{-1}) (±0.3)
La	5.4	27.6	Tb	6.7	28.9
Ce	5.5	27.7	Ho	7.0	29.2
Pr	5.2	27.4	Er	7.4	29.6
Nd	5.1	27.3	Tm	7.2	29.5
Sm	6.0	28.1	Yb	7.3	29.5
Eu	5.9	28.1	Lu	7.4	29.6
Gd	6.6	28.8			

B. Values Measured by NMR (Competition with EDTA (See Text))

La^{3+}/EDTA/DOTP	pD	obsd LaDOTP/LaEDTA	log K_{ML}
1/1/1	7.02	1.01	26.9
1/2/1	7.28	0.98	27.0
1/3/1	7.12	0.62	27.4
1/4/1	7.30	0.63	27.3
1/5/1	7.62	1.00	26.9
1/5/1	7.58	0.75	26.9
			av 27.1 ± 0.2

[a] The values of log α_L and log α_{ML} used to convert the conditional constants to thermodynamic values were 30.92 ± 0.14 and 8.8 ± 0.17, respectively (see text).

methylenephosphonate proton in $LaDOTP^{5-}$ between 2.0 and 2.5 ppm were compared and the $LaDOTP^{5-}/LaEDTA^{-}$ ratio was established for each solution. A conditional constant for the equilibrium $LaEDTA^{-} + DOTP \rightleftharpoons LaDOTP^{5-} + EDTA$ was established for each solution, and given the known protonation and La^{3+} binding constants for EDTA, the formation constant of $LaDOTP^{5-}$ could be established using the protonation constants of $DOTP^{8-}$ and $LaDOTP^{5-}$ as described above. The log K_{ML} value for $LaDOTP^{5-}$ obtained by this method, summarized in Table 2B, was in excellent agreement with the value determined spectrophotometrically.

As a final check of the log K_{ML} values, potentiometry was used to monitor competition between DOTP and DTPA for La^{3+} at high pH values, where La^{3+} exchange between the two ligands appeared to be sufficiently rapid to allow potentiometric measurements. We performed a titration in which HCl was added to a 1/1/1 La^{3+}/DOTP/DTPA solution, initially at a pH of 10.7. The experimental pH curve is shown as the solid line in Figure 3 (top), together with simulated curves (dashed lines) for log K_{ML} = 26, 27.4, and 29. Because the protonation constants of DTPA are significantly lower than those of DOTP, the competition favored $LaDOTP^{5-}$ at the higher pH values and $LaDTPA^{2-}$ at the lower pH values. The most sensitive range to monitor this competitive switch was at pH values between the log K_1^L's of DTPA and DOTP. Between pH 9.5 and 11, the experimental pH curve could be fitted with log K_{ML} = 27.4 ± 0.1. Below pH 9.5, the experimental curve tended to shift toward the calculated curve representing the higher $LnDOTP^{5-}$ stability constant, apparently due to a decrease in the decomplexation rate of $LaDOTP^{5-}$. Another view is given in Figure 3 (bottom), in which the percentage of La^{3+} present as $LaDTPA^{2-}$ is given *versus* the number of equivalents of added titrant. In this plot, the experimental curve overlays the calculated curves for log K_{ML} values of 26, 27.4, and 29. Clearly, the experimental curve follows the log K_{ML} = 27.4 curve well until about 1.5 acid equiv had been added. At this point, dissociation of $LaDOTP^{5-}$ became slower and the experimental data deviated toward the higher stability constant curve. The actual value of log K_{ML} obtained by this method (27.4) supported the data obtained by NMR (27.1) at neutral pH and by colorimetry (27.6) at pH 4.

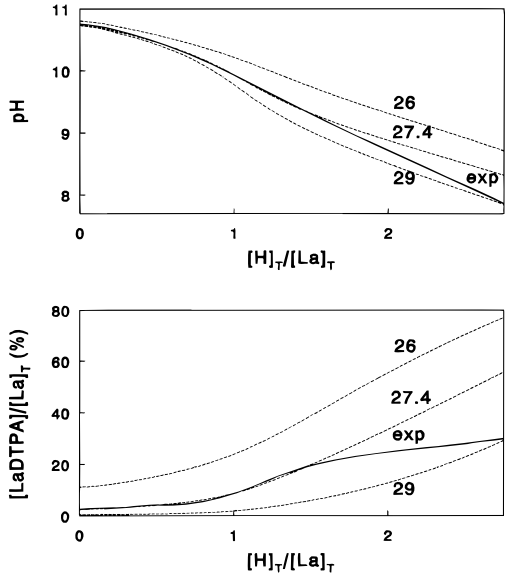

Figure 3. Experimental (solid) and simulated (dashed) potentiometric titration curves for a 1/1/1 $La^{3+}/(Me_4N)_8DOTP/(Me_4N)_5DTPA$ mixture titrated with 0.1 M HCl. The top figure shows the experimental and calculated pH values as a function of added acid while the bottom figure shows the percent $LaDTPA^{2-}$ as a function of added acid. Note that the experimental curve tracks the calculated log K = 27.4 curve for $LaDOTP^{5-}$ up to 1.5 equiv of acid, showing that exchange was rapid above pH ~9.5.

Interaction of $TmDOTP^{5-}$ with Alkali Metal Cations: ^{23}Na NMR. The addition of a variety of alkali metal or ammonium cations to a 15 mM solution of $Na_4HTmDOTP \cdot 3NaCl$ produced an incremental decrease in the observed ^{23}Na-induced shift, depending upon how effectively the added counter-ion competed with existing Na^+ for the sites on $TmDOTP^{5-}$ (Figure 4). Clearly, the tetraalkylammonium cations did not compete effectively with the Na^+ ions already present in solution, while K^+ and NH_4^+ competed more effectively and Cs^+ and Li^+ competed somewhat less effectively. The observed order of alkali ion binding suggests that, of the alkali metal ions, K^+ has the optimal size for site(s) on this SR. The ammonium cation appears to be unique, probably due to its additional hydrogen-bonding capabilities. Previous work by Aime *et al.*[7] has shown that the protonated form of *N*-methylglucamine interacts strongly with $GdDOTP^{5-}$ not only via formation of

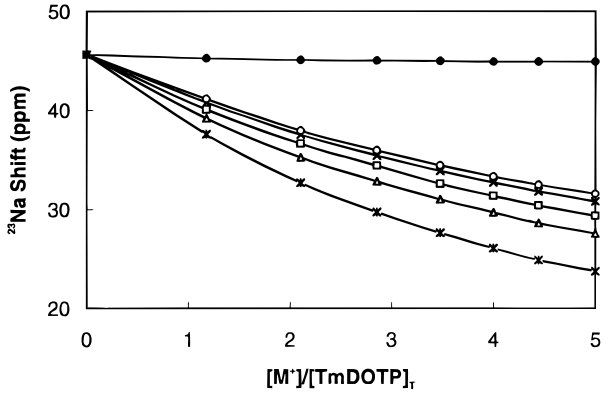

Figure 4. ^{23}Na shift induced by 15 mM $Na_4HTmDOTP{\cdot}3NaCl$ as a function of added alkali or ammonium cations: (●) Me_4N^+ or Et_4N^+; (○) Li^+; (×) Cs^+; (□) Na^+; (△) K^+; and (*) NH_4^+.

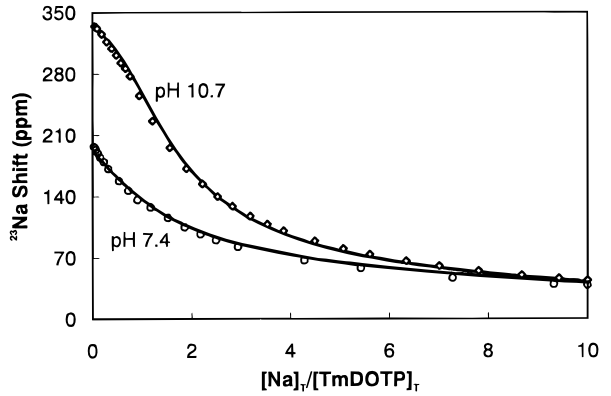

Figure 5. ^{23}Na NMR shift as a function of the $[Na^+]_T/[TmDOTP^{5-}]_T$ ratio at pH 10.7 (◇) and pH 7.4 (○). The solid curves were calculated from the parameters listed in Table 4.

an ion pair but also through hydrogen-bonding of the sugar hydroxyl groups with the bound phosphonates of the complex.

Given this information, we decided to prepare the tetraethylammonium salt of $TmDOTP^{5-}$ and use this for all subsequent cation-binding measurements. Figure 5 illustrates ^{23}Na shifts induced by 15 mM $TmDOTP^{5-}$ at pH 7.4 and 10.7, at 25 °C, as the $Na^+/TmDOTP^{5-}$ ratio was varied from 0.05 to 10. A single ^{23}Na resonance was observed over the entire titration range, indicating that exchange between free Na^+ ions and shift reagent-bound Na^+ ions was fast at this field and temperature. Two points can be made about these data. First, the ^{23}Na shifts were considerably larger at pH 10.7 (where the complex is fully deprotonated) than at pH 7.4 (where the complex is on average monoprotonated). The ^{23}Na shifts were even smaller at lower pH values but approached zero only near pH 4, where the complex was fully protonated.[32] This cation competition effect indicated that protonation of the coordinated phosphonate groups interfered with Na^+ binding, suggesting a possible 1/1 correspondence between the number of Na^+ sites and the number of protonation sites. Second, the magnitude of the observed ^{23}Na shift at the lowest $Na^+/TmDOTP^{5-}$ ratio was well over 300 ppm. This value was nearly as large as some of the largest ^{1}H shifts observed for the fully bound ligand,[5] particularly those protons which are geometrically positioned near the 4-fold symmetry axis of the complex. This suggested that the first Na^+ ion bound to the complex at low $Na^+/TmDOTP^{5-}$ ratios lies near or perhaps along this symmetry axis.

In another experiment, ^{23}Na NMR shifts of a sample initially containing 15 mM $TmDOTP^{5-}$ and 150 mM NaCl at pH 7.4 was measured as a function of added solid NaCl until the total $[Na^+]$ reached 1.8 M. The plot of ^{23}Na paramagnetic shift *versus* $TmDOTP^{5-}/Na^+$ (a ρ plot) was linear over this entire range (see Supporting Information). The slope of this line (480 ppm) equals $\Sigma n_i\Delta_i$, where Δ_i is the bound shift of Na^+ in position i and n_i is the number of Na^+ ions present in that position. Provided that the bound shifts Δ_i could be evaluated, the overall average stoichiometry of the $Na_xTmDOTP$ complex could be determined from this slope.

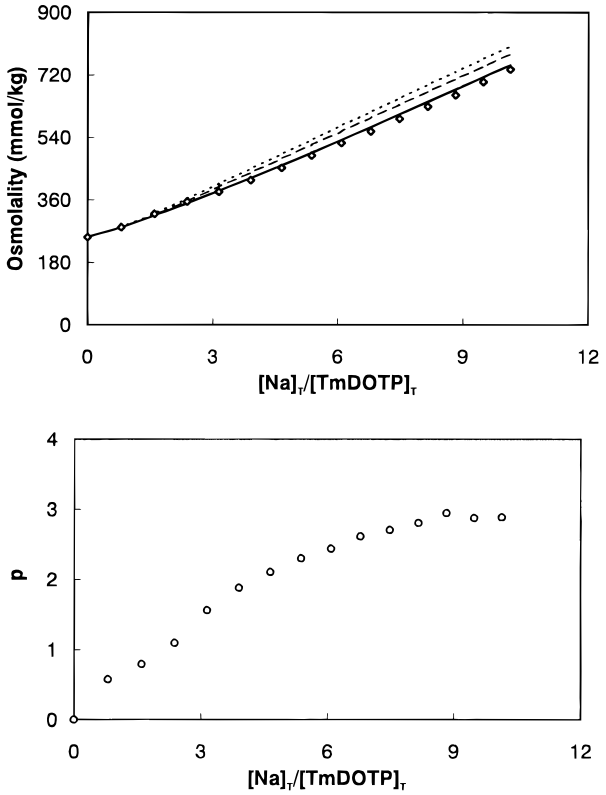

Figure 6. Osmolalities of solutions initially containing 30 mM $(Et_4N)_5$-TmDOTP at pH 12.5 as a function of added NaCl (top). The data (◇) were fit to an equilibrium model including formation of only a 1/1 $NaTmDOTP^{4-}$ adduct (dotted curve), formation of 1/1 and 2/1 adducts (dashed curve), and formation of 1/1, 2/1 and 3/1 adducts as listed in Table 4 (solid curve). The bottom figure shows the average number of Na^+ ions bound to $TmDOTP^{5-}$, p, as a function of $[Na^+]_T/[TmDOTP^{5-}]_T$.

The ^{23}Na spin−lattice relaxation rate (T_1^{-1}) was also sensitive to the $Na^+/TmDOTP^{5-}$ ratio, and the general shape of such curves (see Supporting Information) was similar to that seen for the ^{23}Na shift data (Figure 5). The spin−lattice relaxation rates of other alkali ion nuclei (^{6}Li, ^{7}Li, ^{133}Cs) showed similar behavior.[32] In all cases, the T_1^{-1} *versus* cation concentration curve appeared to be biexponential, indicative of a larger T_1^{-1} value at low alkali cation/$TmDOTP^{5-}$ ratios and a smaller T_1^{-1} value at high alkali cation/$TmDOTP^{5-}$ ratios. None of the curves showed a maximum as reported previously[33] for ^{6}Li relaxation in the presence of $Dy(PPP)_2^{7-}$.

Vapor Pressure Osmometry. The osmolality of solutions containing the SR plus alkali metal salts proved to be sensitive to the identity of the countercation and the amount of excess uncomplexed ions. Figure 6 (top) shows the osmolality of a solution initially containing 30 mM $(Et_4N)_5TmDOTP$ (pH 12.5) and of this solution after the addition of increasing amounts of solid NaCl. These data were used to estimate the average

(32) Ren, J.; Sherry, A. D. *Inorg. Chim. Acta* **1996**, *246*, 1−11.

(33) Ramasamy, R.; Mota de Freitas, D.; Geraldes, C. F. C. G.; Peters, J. A. *Inorg. Chem.* **1991**, *30*, 3188−3191.

number (p) of Na^+ ions coordinated to the SR as a function of the $Na^+/TmDOTP^{5-}$ ratio. A calibration curve was made by measuring the osmolality (Ω_{cal}) of a salt solution with the same starting osmolality ($\Omega_0 = 254$ mOsm/kg) as a function of added NaCl. The experimental osmolality (Ω_{exp}) can be approximated by eq 8. The osmolality difference between the calibration line

$$\Omega_{exp} = \Omega_0 + [Na^+] + [Cl^-] \quad (8)$$

and the experimental data is caused by a decrease in free $[Na^+]$ due to formation of $Na_pTmDOTP$. Since this decrease was equal to the amount of Na^+ present in the bound form, the osmolality difference can be written as eq 9. The *p* values

$$\Omega_{cal} - \Omega_{exp} = \sum_n n[Na_nTmDOTP] = p[TmDOTP]_T \quad (9)$$

$(=(\Omega_{cal} - \Omega_{exp})/[TmDOTP]_T)$ plotted as a function of the $Na^+/TmDOTP^{5-}$ ratio are shown in the bottom panel of Figure 6. At high ratios, the *p* value reached a maximum of 3, corresponding to the number of Na^+ ions bound to the SR under these conditions.

Discussion

Structure and Stability of $LnDOTP^{5-}$ Complexes. The trivalent lanthanide ions form thermodynamically stable and kinetically inert complexes with the tetraazamacrocyclic tetraphosphonate ligand DOTP. Three independent analytical methods were used to measure the stability constant of $LaDOTP^{5-}$, and all three, potentiometry (27.4), NMR (27.1), and colorimetry (27.6), gave similar log K_{ML} values. The values for the remaining lanthanide complexes (determined by colorimetry only) increase by 2 orders of magnitude along the lanthanide series, similar to the trend reported earlier[31] for the $LnDOTA^-$ series. However, unlike the structurally similar $LnDOTA^-$ complexes, the $LnDOTP^{5-}$ complexes form four protonated species between pH 9 and 3, with $HLnDOTP^{4-}$ predominating at pH 7.4. ^{31}P NMR chemical shift titrations indicate that protonation occurs at the coordinated phosphonates, without release of significant amounts of lanthanide ion even at pH 3. A temperature-independent separation (using the Reilley method) of contact and pseudocontact contributions to the ^{31}P shifts for the DOTP complexes of the heavy lanthanide ion series (Tb → Tm) showed that both spin mechanisms were smaller at lower pH values, but the pseudocontact term clearly dominated at all pH values. Thus, the smaller lanthanide(III)-induced shifts of the ^{31}P resonance of the bound phosphonate groups in $TmDOTP^{5-}$ at lower pH values indicate that the chelate structure is somewhat relaxed in the protonated form, and the average position of the phosphorus nuclei in this complex is further away from the paramagnetic center. Conversely, the ^{31}P shifts for the lighter lanthanide complexes (Pr → Eu) were dominated by contact interactions. Thus, the pH-dependent shifts observed for DOTP complexes of ions in this group (as exemplified by the $EuDOTP^{5-}$ data shown in Figure 1) suggest that the Ln^{3+}−ligand bonds (likely the Ln^{3+}−O bonds) are more covalent in the mono- and diprotonated complexes but less covalent in the tri- and tetraprotonated complexes. One might anticipate that protonation of an uncoordinated phosphonate oxygen would increase the negative charge on the coordinated oxygen of the same phosphonate group, thereby increasing the electron density in the Ln^{3+}−O bond. Why this should change, however, during the third and fourth protonation steps remains unclear.

The paramagnetic shifts of all nuclei in $TmDOTP^{5-}$ decrease on an average of 12−13% as the complex becomes protonated between pH 10 and 2, yet only a single species was detected by NMR over this entire pH range. For the $LnDOTA^-$ complexes, two species in slow exchange were observed by NMR: one isomer having a large magnetic susceptibility predominates in the Nd → Lu complexes while a second isomer having a smaller magnetic susceptibility predominates only in the La → Pr complexes.[34−39] Aime[36] has argued that these two species differ only in the position of the bound acetates relative to the macrocyclic ring, with the major isomer (for the majority of the lanthanides) having the square antiprismatic geometry illustrated by the crystal structure[37] of $EuDOTA^-$ and the minor isomer reflecting a prismatic arrangement where the acetate ligands are twisted relative to the nitrogens such that the Ln−O bonds nearly eclipse the Ln−N bonds.[36] Very recently, Bombieri[40] reported in abstract form a crystal structure for $LaDOTA^-$ which showed an "inverted" square antiprismatic arrangement of the carboxylate oxygens relative to the nitrogens. Desreux[34,35,38] has favored a model for the minor structure involving rapid dissociation ⇌ reassociation of the bound carboxylates. The latter model is consistent with two experimental observations. First, the lanthanide complexes formed with the methylacetate analog, DOTMA,[35] also show major and minor species in their ^1H spectra but in this case the major species has the smallest magnetic susceptibility. The lanthanide complexes formed with this ligand are sterically quite demanding, and it would seem reasonable that dissociation of one or more carboxylates would be favored in the $LnDOTMA^-$ complexes relative to the less sterically crowded $LnDOTA^-$ complexes. Also, the addition of inorganic salts to solutions of the $LnDOTA^-$ complexes increases the population of the minor species,[38,39] consistent with but certainly not proof of further release of bound carboxylates. We recently showed that these two hypotheses for the minor isomer cannot be distinguished on the basis of paramagnetic shifts alone.[39]

The magnetic susceptibility difference between the major and minor $LnDOTA^-$ species is quite large, with the average paramagnetic shifts of the minor isomer about 60% of those of the major isomer.[34,36,39] By analogy, one might be tempted to conclude that the smaller shifts observed at lower pH values for the $LnDOTP^{5-}$ complexes with the heavy lanthanide ions may reflect a shift in population from a predominant major species with high magnetic susceptibility at high pH values toward a minor isomer with a lower magnetic susceptibility at lower pH values, all in rapid exchange. However, if one compares the absolute values of the ^1H shifts of the Yb^{3+} complexes of DOTA *versus* DOTP (at pH 10, Table 3), one observes a remarkable agreement between the paramagnetic shifts of the minor $YbDOTA^-$ species and those of $YbDOTP^{5-}$. This is very good evidence for these two species having identical structures. Interestingly, the ^1H shifts observed for $TmDOTP^{5-}$ at pH 10 are consistently about 50% larger than the corresponding proton shifts in the minor form of $TmDOTA^-$ and even larger than most of the corresponding proton shifts of the major form of $TmDOTA^-$ (Table 3). We recently traced the origin of the large paramagnetic shifts observed for $TmDOTP^{5-}$ to an

(34) Desreux, J. F. *Inorg. Chem.* **1980**, *19*, 1319−1324.
(35) Brittain, H. G.; Desreux, J. F. *Inorg. Chem.* **1984**, *23*, 4459−4466.
(36) Aime, S.; Botta, M.; Ermondi, G. *Inorg. Chem.* **1992**, *31*, 4291−4299.
(37) Spirlet, M.-R.; Rebizant, J.; Desreux, J. F.; Loncin, M.-F. *Inorg. Chem.* **1984**, *23*, 359−363.
(38) Jacques, V.; Desreux, J. F. *Inorg. Chem.* **1994**, *33*, 4048−4053.
(39) Marques, M. P. M.; Geraldes, C. F. G. C.; Sherry, A. D.; Merbach, A. E.; Powell, H.; Pubanz, D.; Aime, S.; Botta, M. *J. Alloys Compd.* **1995**, *225*, 303−307.
(40) Bombieri, G. *Abstracts of Papers*; COST Working Group on *Synthesis and Physicochemical Studies of Lanthanide and Transition Metal Chelates of Relevance to MRI*, Torino, Italy, 1994.

Table 3. Comparison of the Paramagnetic Shifts of $LnDOTA^-$ Complexes with Those of the Fully Deprotonated Forms of Some $LnDOTP^{5-}$ Complexes

ligand proton[a]	$YbDOTA^-$ minor species		$YbDOTP^{5-}$ pH 10[a]	$TmDOTA^-$ minor/major species[d]		$TmDOTP^{5-}$ pH 10[a]
H_1	−37.2[b]	−38.3[c]	−34.6	−134.2	−205.8	−193.7
H_2	13.2	11.2	16.4	45.2	52.1	72.7
H_3	8.6	9.9	11.9	60.3	68.0	92.8
H_4	84.7	86.3	89.9	366.3	468.2	513.6
H_5	−61.2	−61.9	−66.2	−240.8	−358.9	−398.9
H_6	−32.3	−33.9	−27.4	−113.8	−170.7	−155.7

[a] The protons are designated as in ref 5. H_1−H_4 correspond to ethylene protons, while H_5 and H_6 correspond to acetate or methylenephosphonate protons; 25 °C. [b] From ref 34; −2 °C. [c] From ref 36; 0 °C. [d] From ref 39; 20 °C.

abnormally high crystal field coefficient, $A_2^0\langle r^2\rangle$, for this complex.[41] The unique magnetic properties of $TmDOTP^{5-}$ is one of the factors that make this charged complex an unusually good aqueous shift reagent for biological cations.[1,6,14−22]

Complexes Formed between Alkali Metal Ions and $TmDOTP^{5-}$. All ^{23}Na NMR shift titration curves and osmometric data collected at high pH (where $TmDOTP^{5-}$ is fully deprotonated) were fit to several ion−SR binding models. The osmolality data (Figure 6, bottom) indicate that three Na^+ ions are bound whenever the $Na^+/TmDOTP^{5-}$ ratio is above ∼10. Several characteristics of the ^{23}Na chemical shift *versus* $Na^+/TmDOTP^{5-}$ curves shown in Figure 5 are also consistent with multiple Na^+-binding sites on the SR. At low $Na^+/TmDOTP^{5-}$ ratios (where most of the Na^+ would be bound as a 1/1 complex), an unprecedentedly high ^{23}Na NMR shift was observed, reflecting a fully bound shift of at least 400 ppm. This value indicates that the first Na^+ binding site (position A) must be located on or near the principal magnetic axis of $TmDOTP^{5-}$. The ^{23}Na NMR shift data further show that increasing the $Na^+/TmDOTP^{5-}$ ratio above 1 resulted in a significantly lower paramagnetic shift. This indicates that subsequent Na^+ ions bind at a different geometrical position on the SR (the B-positions) with a lower bound shift. This smaller bound shift likely reflects a binding position with a substantially larger angle with respect to the principal magnetic axis of the complex, either with the first Na^+ ion still bound to the central position A or with this ion displaced by the binding of subsequent Na^+ at the B-position(s). Many of our data favor the latter model. First, an optimal fit of the ^{23}Na shift data of Figure 5 could only be obtained for such a model, including at least three B-sites. Further evidence is given by data[32] on competition between Na^+ and Ca^{2+} for complexation with $TmDOTP^{5-}$: Addition of Ca^{2+} to a solution containing Na^+ and $TmDOTP^{5-}$ in an equimolar ratio resulted in complete reversal of the ^{23}Na shift at a $Ca^{2+}/TmDOTP^{5-}$ ratio of 1. This indicates that Na^+ cannot bind to the B-sites when a single Ca^{2+} is bound, likely at a position similar to the A binding position for Na^+.

The ρ plot (see Supporting Information) is also consistent with a three-Na^+-binding-site model. These data were obtained at high $Na^+/TmDOTP^{5-}$ ratios (>10) where at least two, but more likely either three or four Na^+ ions are coordinated. The slope of this line was 480 ppm, a value that is similar to the fully bound shift of a Na^+ ion at site A. If the A- and B-sites could be occupied simultaneously, then either the number of Na^+ ions in the B-site (n_B) or their bound shift (Δ_B) must be small, because the slope then originates almost completely from the single Na^+ ion in the A-position. Both cases, however, are in contradiction with the shift data of Figure 5, which clearly shows a significant contribution of B-bound Na^+ to the chemical shift at high $Na^+/TmDOTP^{5-}$ ratios. This means that for the ρ plot, the A-site must be unoccupied and the slope reflects Na^+ binding only in the B-positions. This leads us to the following model, where L = $TmDOTP^{5-}$:

$$Na^AL \rightleftharpoons L \rightleftharpoons Na^BL \rightleftharpoons (Na^B)_2L \rightleftharpoons \rightleftharpoons (Na^B)_xL$$

Upon addition of Na^+ to $TmDOTP^{5-}$, the first Na^+ ion binds preferably to the central position A. However, binding of more than one Na^+ ion is only possible at the B-sites, so competition favors Na^+ binding at the B-sites at high Na/L ratios.

The exact number (x) of B-sites is difficult to determine. Fitting the data illustrated in Figure 5 gives a good fit for both $x = 3$ and $x = 4$. Since there are four protonation steps for $TmDOTP^{5-}$ (see above) that are fairly close to each other, it is reasonable to assume that $x = 4$ is also the maximum for Na^+ binding. The only experimental technique that is more sensitive to the total number of Na^+ ions binding to $TmDOTP^{5-}$ is osmometry. Figure 6 (bottom) shows the average number of Na^+ ions binding to the SR as a function of the $Na^+/TmDOTP^{5-}$ ratio. Under these conditions, a limiting (average) number of 3 was observed. Compared with that for the $x = 4$ model, the Δ_b value for the $x = 3$ model (162 ppm) also agrees better with the slope of the ρ plot (480 ppm/3 = 160 ppm). However, this does not exclude the formation of the species with $x = 4$ at higher $TmDOTP^{5-}$ concentrations or higher $Na^+/TmDOTP^{5-}$ ratios. Overall, it is concluded that at least three Na^+ ions bind to $TmDOTP^{5-}$ at high $Na^+/TmDOTP^{5-}$ ratio, but that coordination of a fourth ion is also plausible. Optimized $Na_xTmDOTP$ stability constants for the pH 10.7 ^{23}Na shift curve of Figure 5 assuming a single A-site and three or four B-sites are presented in Table 4. It was assumed that the bound shifts of all Na^+ ions at B-sites were equal and that the stepwise $(Na^B)_xL$ binding constants decreased only in a statistical manner with each additional bound Na^+ ion.

At physiological pH (7.4), the observed ^{23}Na shifts were generally lower because of H^+ competition. Previous data[32] showed that the ^{23}Na shifts decrease gradually between pH 9 and 4, the same pH range where four protonations were detected by potentiometry. Therefore, it seems probable that protons and Na^+ ions compete for the same B-sites on the bound phosphonates. Accordingly, the pH 7.4 ^{23}Na shift data (and relaxation rate data, not shown) were fitted to this model by including the $TmDOTP^{5-}$ protonation constants (Table 1). Since Na^+ binding at the A- and B-sites appears to be competitive, it was assumed that protonation of $Na^ATmDOTP^{4-}$ does not occur at physiological pH. As discussed above, the structure of $TmDOTP^{5-}$ relaxes upon protonation and the Tm−P distances become larger. This could also alter the A-site and provide for poorer accommodation of a Na^+ ion in this position. Binding of Na^+ to the B-sites may have an effect on the structure of the complex similar to that of protonation, thus preventing the formation of species with Na^+ ions in both the A- and the B-positions. Binding constants for the mixed $(Na^B)_xH_yTm$-DOTP species are also listed in Table 4 but are somewhat less accurate due to lack of constraints.

The approximate composition of SR used in most *in vivo* ^{23}Na NMR studies to date has been $Na_4HTmDOTP{\cdot}3NaOAc$.[19−22] A 80 mM stock solution of SR with this formulation has a measured osmolality of 640 mOsm/kg and a ^{23}Na chemical shift of 62 ppm (relative to saline) at 25 °C. The concentrations of the species in this 80 mM stock solution, estimated from the Na^+-binding constants given in Table 4, were given in paren-

(41) Ren, J.; Sherry, A. D. *J. Magn. Reson.* **1996**, *111* (Series B), 178−182.

Table 4. Binding Constants, Protonation Constants, and Limiting ^{23}Na Shifts and Relaxation Rates for the Binding Model Derived from the ^{23}Na NMR Data Shown in Figure 5 (L = $TmDOTP^{5-}$)

equilibrium[a]	log K ($x = 3$)	log K ($x = 4$)
$[Na^AL]/[Na][L]$	2.58 ± 0.17	2.57 ± 0.17
$[Na^BL]/[Na][L]$	1.78 ± 0.11	1.77 ± 0.11
$[(Na^B)_2L]/[Na][Na^BL]$	1.65 ± 0.10	1.64 ± 0.10
$[(Na^B)_3L]/[Na][(Na^B)_2L]$	1.48 ± 0.09	1.47 ± 0.09
$[(Na^B)_4L]/[Na][(Na^B)_3L]$		1.17 ± 0.07
$[Na^BHL]/[H][Na^BL]$	7.48 ± 0.15	7.48 ± 0.15
$[Na^BH_2L]/[H][Na^BHL]$	6.84 ± 0.24	6.84 ± 0.24
$[(Na^B)_2HL]/[H][(Na^B)_2L]$	7.45 ± 0.14	7.45 ± 0.14
$[(Na^B)_3HL]/[H][(Na^B)_3L]$	6.43 ± 0.26	6.43 ± 0.26
$AF = [\sum(\Delta_{obs} - \Delta_{cal})^2/\sum\Delta_{obs}^2]^{1/2}$	3.4%	3.3%
$AF = [\sum(T_{1obs}^{-1} - T_{1cal}^{-1})^2/\sum(T_{1obs}^{-1})^2]^{1/2}$	7.0%	6.9%

species[a]	Δ (ppm) ($x = 3$)	T_1^{-1} (s^{-1}) ($x = 3$)	Δ (ppm) ($x = 4$)	T_1^{-1} (s^{-1}) ($x = 4$)
Na^AL	420 ± 10	1011 ± 70	423 ± 9	1000 ± 68
$(Na^B)_xH_yL$	162 ± 5	367 ± 29	141 ± 5	350 ± 25

[a] A and B denote binding sites A and B, respectively; the charges are omitted for clarity.

theses as follows (mM): OAc^- (240), $Na_3TmDOTP^{2-}$ (34.0), $Na_3HTmDOTP^-$ (36.6), $Na_2TmDOTP^{3-}$ (3.4), $Na_2HTmDOTP^{2-}$ (3.8), $NaTmDOTP^{4-}$ (1.7), $NaHTmDOTP^{3-}$ (0.3), and Na^+_{free} (332). The sum of these individual species concentrations, 652 mM, agreed quite favorably with the measured osmolality. This indicates that a significant fraction (69%) of the total Na^+ in such a stock solution is in a bound form, thereby yielding a solution osmolality significantly lower than that originally anticipated. Furthermore, the calculated ^{23}Na NMR shift based upon the mole fraction of each sodium species and the limiting shift of each species shown in Table 4 was 66 ppm, a value that was close to the observed ^{23}Na shift of 62 ppm.

Although the unique binding site A appears to have the highest affinity for Na^+ (log $K = 2.58$) and the largest fully bound shift (420 ppm), the amount of Na^+ bound at this site during a typical biological experiment is inconsequential. Whenever $[Na^+]_T$ is 7−10-fold greater than $[TmDOTP^{5-}]$, the Na^+ ions are bound at the B-sites located further away from the principal axis of symmetry. Site A provides a distinct geometric advantage. With the average position of Na^+ lying about 26° off the 4-fold symmetry axis of the complex and ∼3.7 Å from the Tm^{3+} cation, the bound shift of Na^+ at this site is more than 400 ppm. The B sites are geometrically less advantageous (34° from the axis and ∼4.5 Å from the paramagnetic center), but there are more of them. A maximum of three B-sites, each having a bound shift near 160 ppm, has about the same shift contribution as a single Na^+ bound at the A-site. Thus, any design strategies to improve upon $TmDOTP^{5-}$ as an SR for Na^+ should involve either restricting Na^+ to a single (A) binding region on or near the 4-fold symmetry axis of the complex or increasing the number of B-sites.

Acknowledgment. This research was supported in part by grants from the Robert A. Welch Foundation (AT-584) and the NIH Biotechnology Research Program (RR-02584) to A.D.S. C.F.G.C.G. and M.M.C.A.C. acknowledge support from the JNICT (Portugal) through Grant PBIC/S/SAU/1623/92.

Supporting Information Available: Plots of ^{31}P LIS/$\langle S_z\rangle$ *versus* $D/\langle S_z\rangle$ for the heavy $LnDOTP^{5-}$ complexes (Ln = Tb → Yb) at pH 3 and 10 showing that the paramagnetic shift at the phosphorus nucleus for these complexes is dominated by the pseudocontact term at both pH values, ^{23}Na spin−lattice relaxation rates as a function of $[Na^+]_T/[TmDOTP^{5-}]_T$ at pH 10.7 and 7.4 along with a fit of the raw data to the binding model described in the text, ^{23}Na shifts induced by 15 mM $TmDOTP^{5-}$ as a function of added Na^+ (where the $[Na^+]$ was always at least 2-fold higher than $[TmDOTP^{5-}]$), and the distribution of Na^+ ions in sites A and B on $TmDOTP^{5-}$ as calculated by the equilibrium model of Table 4 (4 pages). Ordering information is given of any current masthead page.

IC9600590